

Optic Nerve Degeneration in a Murine Model of Juvenile Ceroid Lipofuscinosis

Rebecca M. Sappington,¹ David A. Pearce,^{2,3} and David J. Calkins^{4,5}

PURPOSE. To investigate optic nerve degeneration associated with CLN3 deficiency in a murine model of juvenile neuronal ceroid lipofuscinosis (Batten disease).

METHODS. Using light and electron microscopy, the density and diameter of axons and the thickness of myelin in optic nerve were compared between age-matched *cln3* knock-out (*cln3*^{-/-}) and wild-type (129ev/TAC) mice. Western blot analysis was used to assay expression of Cln3 in mouse and primate retina and optic nerve.

RESULTS. Morphologically identified mast cells were present in the meningeal sheaths surrounding the *cln3*^{-/-} nerve and in the nerve itself. The *cln3*^{-/-} optic nerve exhibited an overall loss of uniformity and integrity. Axon density in *cln3*^{-/-} optic nerve was only 64% of that in wild-type optic nerve ($P < 0.01$). Accounting for differences in axon density, the diameter of axons in *cln3*^{-/-} optic nerve was 1.2 times greater than in wild-type optic nerve ($P < 0.01$). Electron micrographs revealed large spaces between axons and 32% thinner myelin surrounding axons in *cln3*^{-/-} mice than in wild type ($P < 0.01$). Western blot analysis demonstrated that Cln3 was expressed in retinas and optic nerves of mouse and primate.

CONCLUSIONS. The presence of apparent mast cells in *cln3*^{-/-} optic nerve suggests compromise of the blood-brain barrier. The absence of Cln3 causes loss of axons, axonal hypertrophy, and a reduction in myelination of retinal ganglion cells. Furthermore, expression of CLN3 in mouse and primate optic nerve links degeneration to loss of Cln3. (*Invest Ophthalmol Vis Sci.* 2003;44:3725-3731) DOI:10.1167/iovs.03-0039

Juvenile neuronal ceroid lipofuscinosis (Batten disease) is a pediatric neurodegenerative disease marked by early vision loss, seizures, psychomotor dysfunction, and premature death. Postmortem examination reveals severe retinal, cortical, and cerebellar atrophy accompanied by the accumulation of autofluorescent, lysosomal storage material. Subunit c of mitochondrial adenosine triphosphate (ATP) synthase is a major component of these deposits.¹⁻³ Batten disease is associated

with numerous mutations in the *cln3* gene, which encodes a 438-amino-acid polypeptide with an apparent molecular weight of 48 kDa.⁴ The encoded protein CLN3 is highly conserved across species and is ubiquitously expressed, with 5 to 10 predicted membrane-spanning domains.^{4,5} Localization studies are conflicting, with reports of lysosomal, mitochondrial, Golgi, and nuclear localization.⁶⁻¹¹ To date, the function of CLN3 is unknown; however, the highly conserved nature of this protein allows for investigation of its function in many model systems. In mice, Cln3 colocalizes with synaptic vesicle proteins, suggesting a role for CLN3 in trafficking of synaptic vesicles.¹²⁻¹⁴ In yeast, loss of BTN1, the yeast homologue of CLN3, reduces lysosomal pH, and cultured cells derived from patients also demonstrate altered lysosomal pH, suggesting a role for CLN3 in pH homeostasis.^{15,16}

Pathologic changes in Batten disease manifest early in the retina and accompany complete loss of vision. Postmortem investigation has revealed severe retinal degeneration with accumulation of granular, autofluorescent material.¹⁷ Cell death in the retina appears to be neuronal, with complete loss of the outer retina, including both the nuclear (cell bodies) and the plexiform (synaptic) layer. Although the inner nuclear and plexiform layers and the ganglion cell layer appear relatively intact, the cells remaining are most likely glial (Müller cells and astrocytes).¹⁸ Thus, Batten disease induces loss of both synaptic and neuronal layers in the retina. Funduscopy also has revealed thinning of retinal vasculature and atrophy of the optic nerve head.¹⁹ An earlier investigation of retinal disease in a *cln3* knock-out (*cln3*^{-/-}) mouse model of Batten Disease has revealed thinning of the inner and outer plexiform layers.²⁰

We investigated density and diameter of axons and the thickness of myelin surrounding the axons in optic nerve of the same *cln3*^{-/-} mouse. We observed a decrease in the number of axons comprising the optic nerve; however, the diameter of the axons increased. We believe this indicates a general loss of the ganglion cell population accompanied by hypertrophy of ganglion cell axons. In addition, we observed a reduction in the thickness of myelin sheathing surrounding individual axons. These changes could result from abnormal development or degenerative mechanisms. We propose a developmental hypothesis for reduced myelination based on the possible role of CLN3 in pH homeostasis.

METHODS

Animals and Tissue Preparation

All protocols involving the use of mice adhered to the regulations set forth in the ARVO Statement for the Use of Animals in Ophthalmic and Vision Research.

Murine Optic Nerve. *Cln3*^{-/-} mice were created on a 129ev/TAC background (also known as 129S6), as previously described.^{14,20,21} Briefly, a PGK neomycin cassette was inserted into a plasmid designed to delete and replace exons 1 to 6 of the *cln3* gene. As shown previously and reconfirmed in this study, the *cln3*^{-/-} mouse demonstrates loss of Cln3 protein expression. *Cln3*^{-/-} and age-matched wild-type mice ($n = 4$) were anesthetized and perfused

From the ¹Interdepartmental Graduate Program in Neuroscience, the ²Center for Aging and Development, the Departments of ³Biochemistry and Biophysics and ⁴Ophthalmology, and the ⁵Center for Visual Science, University of Rochester Medical Center, Rochester, New York.

Supported by National Institute of Neurological Disorders and Stroke Grant NS40580 (DAP), the Sloan Foundation (DJC), the EJLB Foundation (DAP), the Schmitt Foundation (DAP/DJC), Research to Prevent Blindness (DJC), and the JNCL Research Fund (DJC/DAP).

Submitted for publication January 14, 2003; revised March 20 and April 8, 2003; accepted April 21, 2003.

Disclosure: R.M. Sappington, None; D.A. Pearce, None; D.J. Calkins, None

The publication costs of this article were defrayed in part by page charge payment. This article must therefore be marked "advertisement" in accordance with 18 U.S.C. §1734 solely to indicate this fact.

Corresponding author: David J. Calkins, University of Rochester Medical Center, Department of Ophthalmology, 601 Elmwood Avenue, Box 314, Rochester, NY 14642; calkins@cvs.rochester.edu.

with 4% paraformaldehyde+2.5% glutaraldehyde in phosphate buffer (pH 7.4). The optic nerve ($n = 8$) was immediately placed in 4% glutaraldehyde overnight at 4°C. Optic nerve segments were then rinsed in cacodylate buffer and postfixed in 1% osmium (OsO_4) in cacodylate buffer for 30 minutes. Segments were then rinsed in cacodylate buffer, dehydrated in graded alcohol solutions, and embedded in Epon-Araldite at 60°C for 72 hours.

Western Blot Analysis. Tissues for Western blot analysis were obtained as fresh-frozen specimens from various laboratories at the University of Rochester Medical Center. For Cln3 expression in brain, we procured fresh whole brain from wild-type (129ev/TAC) mouse, *cln3*^{-/-} mouse, rat, and vole (a small rodent); cerebellum from the Old World primate, *Macaca fascicularis*; and frozen protein lysate from human brain. For Cln3 expression in the retina, we procured fresh retina and optic nerve from wild-type (129ev/TAC) mouse and *Macaca fascicularis*. Tissue samples were homogenized in a buffer containing: 2-(*N*-morpholino)ethane sulfonic acid (MES; pH 6.75), 1:1000 proteinase inhibitors (PIC I and PIC II), and 1:20 phenylmethylsulfonyl fluoride (PMSF; in isopropanol). After homogenization, tissue samples were centrifuged and protein lysates collected as the resultant supernatant. Bradford protein assays were conducted to determine the concentration of protein in each lysate. Protein lysates of 15 to 25 μg /well were separated electrophoretically through a gradient gel of 6% to 15% polyacrylamide.

Antibodies

For protein detection by Western blot, we used a rabbit polyclonal antibody (Q438) specific for residues 250 to 264 of Cln3 (1:1000). Antibodies were generated by and obtained as a gift from Michael J. Bennett, PhD, Children's Medical Center of Dallas.¹¹

Quantification of Light Microscopy

For light microscopy, semithin sections of optic nerve were cut at 2 μm , counterstained with toluidine blue, and photographed under a microscope (Provis AX70; Olympus, Melville, NY) digitally interfaced with a semicooled charge-coupled device (CCD) camera (RT-Spot; Diagnostic Instruments, Sterling Heights, MD) and image capture software (ImagePro; MediaCybernetics, Silver Spring, MD). Three regions from each semithin section were randomly chosen for quantification of axon density and diameter. We measured axon density by applying a square grid of 25 μm per side to 31 randomly chosen regions and performing a manual count of all complete axons in each grid. Axon density was then determined as the number of axons in a 50- μm^2 area. Axon diameter was measured by tracing the perimeter of 50 neighboring axons in several samples of the semithin sections for a total of 602 axons. For diameter measurements, an equal number of axons were measured in wild-type and *cln3*^{-/-} specimens to account for differences in axon density.

Quantification of Electron Microscopy

For electron microscopy, serial ultrathin sections were cut at 70 nm and photographed under an electron microscope (model 7100; Hitachi America, San Jose, CA). Four montages consisting of $\times 7000$ images each were obtained from select sections, yielding a total of 128 photographs. To measure myelin thickness, we overlaid a montage of adjacent square grids of 5 μm per side on the electron micrographs. Width measurements for myelin sheathing were obtained every time a vertical grid line encountered myelin. For most axons, two encounters were measured.

Statistical Analysis

For statistical comparison between wild-type and *cln3*^{-/-} mice, we pooled data across individual animals within each group to calculate mean \pm SEM. For most measurements, the data were not appreciably skewed or kurtotic and reasonably approximated by a normal distribution,

as verified with the Kolmogorov-Smirnov normality test. Comparisons for these measurements were made using the Student's *t*-test, and $P < 0.05$ was considered statistically significant. The distributions of measurements of axon diameter were naturally skewed toward smaller values, because in mice larger ganglion cells and axons are less frequently encountered. For these, we used the Mann-Whitney rank-sum test for comparing means, because this test does not rely on a normal distribution of the data.

RESULTS

Gross Pathology

Semithin sections of optic nerve from *cln3*^{-/-} mice (100 \times) stained with toluidine blue revealed metachromatically stained granules within the cytoplasm of large cells contained within the meningeal sheaths surrounding the nerve (Figs. 1A, 1B) and in the nerve itself (Fig. 1C). Often, these granules surrounded a large, distended, and darkly stained nucleus (Fig. 1A). These cells meet the standard morphologic criteria for identification of mast cells. Specifically, the cells demonstrate the same purplish-red hue that mast cells assume with toluidine blue staining, which contrasts sharply with the blue shade of surrounding axons.^{22,23} Indeed, the identification of mast cells in meninges of the nerve is not unexpected because the cells normally are associated with connective tissue. Also, mast cells generally do not cross the blood-brain barrier, but can do so during inflammation.²² The identification of mast cells in glutaraldehyde-fixed tissue (such as that used in our study) is generally made with basic histologic stains,²³ because such heavy fixation precludes the use of cell-specific markers.

Compared with optic nerve from wild-type mice (Fig. 2A), *cln3*^{-/-} optic nerve exhibited an overall loss of uniformity and integrity (Fig. 2B). Specifically, axons in wild-type optic nerve were generally uniform in shape and packed together tightly to form the fibers of the nerve (Fig. 2A). In contrast, spacing between axons of *cln3*^{-/-} optic nerve increased to give an overall impression of loose axonal packing, which suggests loss of axons (Fig. 2B). Individual axons of *cln3*^{-/-} optic nerve also exhibited distention and distortion that resulted in a departure from the circular morphology of normal axons (Fig. 2B).

Light Microscopy and Quantification of Pathologic Morphology

To characterize loss of uniformity and integrity in *cln3*^{-/-} optic nerve, we compared axon density and axonal diameter in *cln3*^{-/-} and wild-type specimens. We measured axon density as described in the Methods section. In support of qualitative observations, axon density was reduced in *cln3*^{-/-} optic nerve (0.136 ± 0.004 axons/ μm^2) compared with wild-type optic nerve (0.212 ± 0.006 axons/ μm^2). This 36% reduction is highly significant ($t_{(30)} = 9.34$, $P < 0.01$; Fig. 3A). We also compared the cross-sectional area of semithin sections of the optic nerve. We found that the nerve of the *cln3*^{-/-} mouse was consistently smaller in area (0.092 ± 0.001 mm^2) than the wild-type nerve (0.095 ± 0.001 mm^2). This difference is significant across multiple sections ($t_{(10)} = 4.54$, $P < 0.01$).

Accounting for differences in axon density as described, the diameter of axons in *cln3*^{-/-} optic nerve was consistently greater (1.533 ± 0.049 μm) than in wild-type optic nerve (1.262 ± 0.049 μm). Both distributions failed the Kolmogorov-Smirnov normality test because of their obvious and natural skew toward smaller diameters (wild-type: $P < 0.01$; *cln3*^{-/-}: $P < 0.01$). Because of this, we applied the Mann-Whitney rank-sum test, which makes no assumption

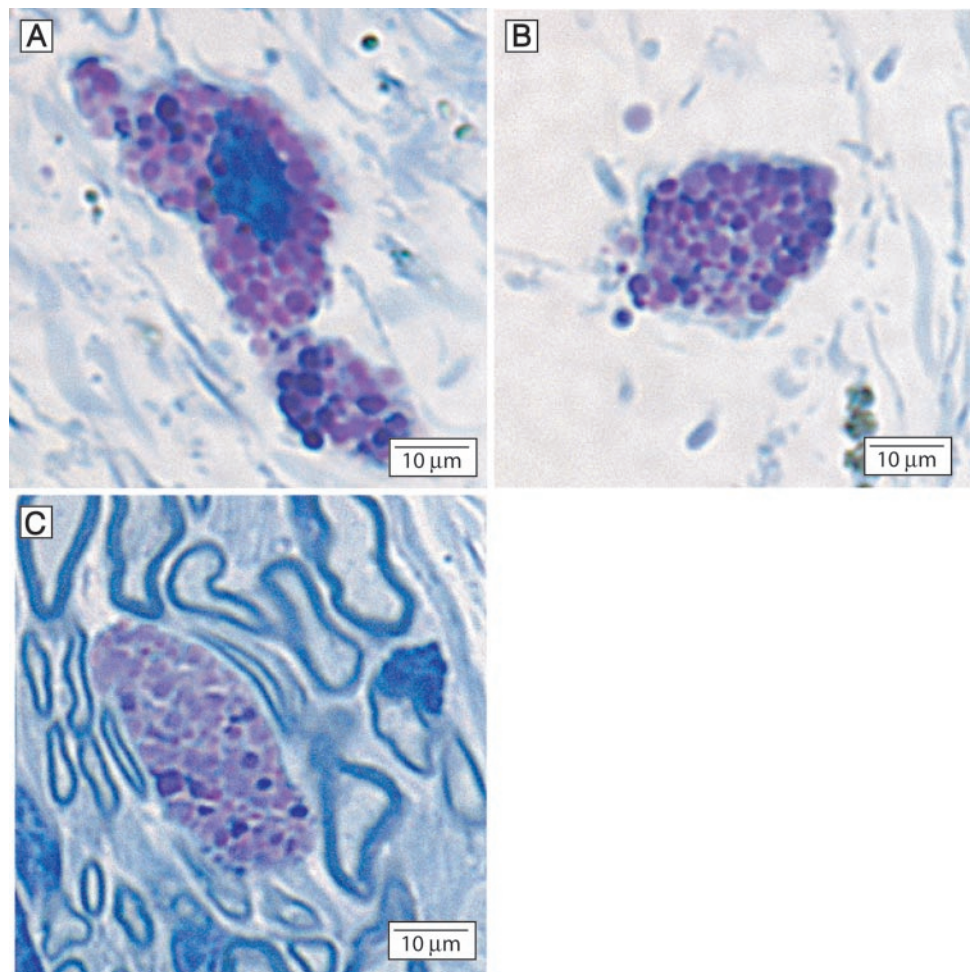


FIGURE 1. Gross pathology of *cln3*^{-/-} optic nerve includes infiltration of mast cells, a characteristic of large-scale inflammation and blood-brain-barrier compromise. (A-C) Semithin sections of optic nerve from *cln3*^{-/-} mouse stained with toluidine blue revealed the presence of mast cells in the meningeal sheaths surrounding the nerve (A, B) and in the nerve itself (C). When exposed to toluidine blue, mast cells assumed a purplish-red hue, as opposed to the blue hue of most other cells (A-C).^{22,23} Magnification, $\times 100$.

tions about the underlying statistical distribution. The difference in axon diameter is highly significant ($t_{(601)} > 100,000$, $P < 0.01$; Fig. 3B). We interpret this finding as fewer axons of small diameter in the *cln3*^{-/-} optic nerve. This interpretation is supported by the sharp decrease in axons of diameter less than 2 μm .

Electron Microscopy and Quantification of Pathologic Morphology

Loss of structural integrity at the level of individual axons is likely to underlie the eventual decrease in the density of axons in *cln3*^{-/-} optic nerve. Therefore, we investigated changes in the morphology of individual axons that may lead to or precede loss of axons. Electron micrographs of *cln3*^{-/-} optic nerve revealed pathologic changes consistent with those documented in the semithin sections (Fig. 4, compare with Fig. 2B). Specifically, *cln3*^{-/-} optic nerve contained larger spaces between axons than wild-type optic nerve, and the myelin sheathing on individual axons appeared disrupted (Figs. 4A, 4B). To quantify pathologic changes in myelin sheathing, we overlaid a montage of adjacent square grids of 5 μm per side on the electron micrographs. Measurements for myelin sheathing were obtained every time a grid line encountered myelin for a total of more than 4000 measurements. These measurements revealed that the thickness of myelin surrounding axons in *cln3*^{-/-} mice is significantly reduced: $0.060 \pm 0.001 \mu\text{m}$ for *cln3*^{-/-} versus $0.088 \pm 0.001 \mu\text{m}$ for wild-type ($t_{(4138)}$

$= 18.02$, $P < 0.01$; Fig. 4C). No significant differences existed between myelin measurements in the peripheral and central portions of both *cln3*^{-/-} and wild-type optic nerve.

Cln3 Protein Expression

To reliably associate optic nerve degeneration with loss of Cln3, we assayed Cln3 expression in brain, retina, and optic nerve across multiple species. Q438, the anti-Cln3 antibody used in our study, localized Cln3 to the nucleus and cellular membranes in a previous reports.¹¹ Our Western analyses confirmed expression of Cln3 in rodent and nonhuman primate brain, CLN3 in human brain (Fig. 5A), and Cln3 in mouse and nonhuman primate retina (Fig. 5B). Most important, Cln3 was expressed in both mouse and non-human primate optic nerve (Fig. 5C).

DISCUSSION

We examined optic nerve tissue from *cln3*^{-/-} mice, a model of juvenile ceroid lipofuscinosis (Batten disease), and report pathologic findings consistent with compromise of the blood-brain barrier (Fig. 1), loss of axons (Figs. 2, 3), axonal hypertrophy (Figs. 2, 3), and a reduction in myelination of retinal ganglion cell axons (Fig. 4). Furthermore, the novel finding that Cln3 is present in optic nerve links the absence of Cln3 with optic nerve degeneration (Fig. 5). We conclude that the severe retinal degeneration characteristic of Batten disease and

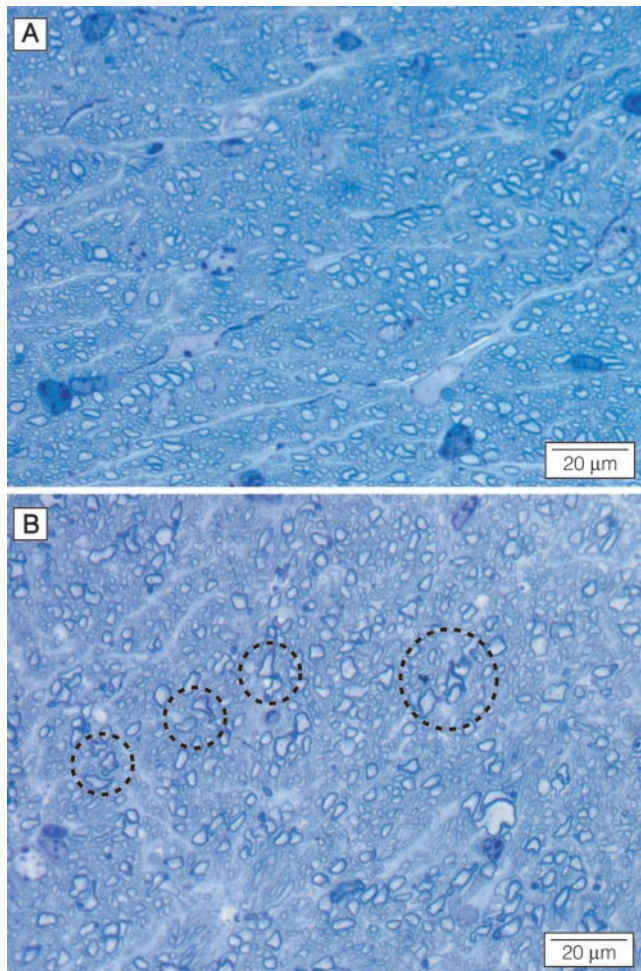


FIGURE 2. Pathologic changes in the *cln3*^{-/-} optic nerve included distention and distortion of individual axons. (A) Semithin section of optic nerve from wild-type mouse stained with toluidine blue demonstrated the morphology of a healthy, intact optic nerve. Individual axons were generally uniform in shape and packed together tightly to form the fibers of the nerve. (B) Toluidine blue staining of a semithin section of optic nerve from *cln3*^{-/-} mouse revealed an overall loss of nerve integrity with apparent loosening of axonal packing, which suggests loss of axons. Individual axons also exhibited pathologic changes in morphology. Disease in individual axons was characterized by axonal distention and distortion that resulted in a departure from the circular morphology of normal axons (dashed black circles). This loss of uniformity at the level of individual axons probably underlies the overall loss of uniformity and nerve integrity. Magnification, $\times 100$.

previously reported in the same *cln3*^{-/-} mouse,²⁰ correlates with severe degeneration of the optic nerve.

Mast Cells Present in Optic Nerve

The first striking morphologic abnormality of the *cln3*^{-/-} optic nerve was the presence of apparent mast cells in the meningeal sheaths (Figs. 1A, 1B) surrounding the nerve and in the nerve itself (Fig. 1C). Such cellular infiltration of mast cells suggests a compromise of the blood-brain barrier. This compromise would most likely occur at the level of the retina, because dye leakage from retinal circulation during fluorescein angiography and thinning of retinal vasculature has been noted in patients with Batten disease.¹⁹ Furthermore, studies of brain tissue from the same *cln3*^{-/-} mouse¹⁴ and sera from patients with Batten disease²⁴ reveal the presence of autoantibodies

against an isoform of glutamic acid decarboxylase (GAD65). These results are consistent with a hypothesis that Batten disease includes an inflammatory component. Ongoing studies in our laboratories are exploring this possibility.

Loss of Axons and Axonal Hypertrophy

Morphologic assessment of the *cln3*^{-/-} optic nerve reveals overall loss of uniformity and integrity (Figs. 2A, 2B), which contrasts sharply with the uniform shape and integrity of the

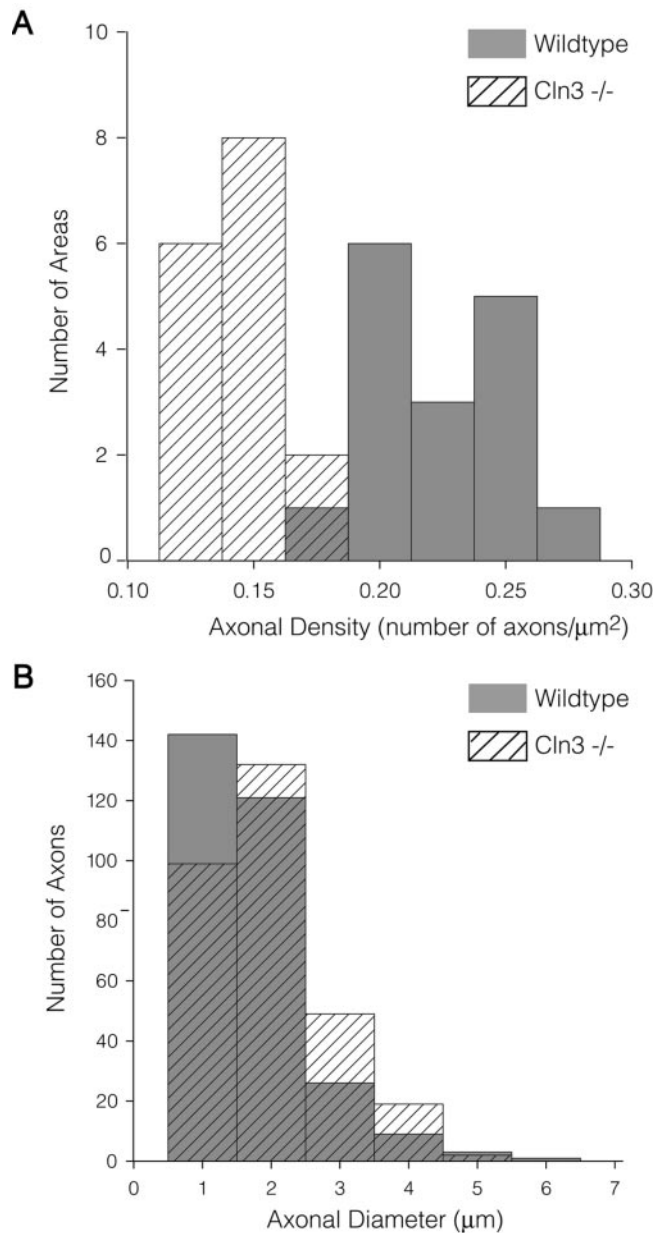


FIGURE 3. Reduced axonal density but greater diameters in *cln3*^{-/-} optic nerve. (A) Axon density was reduced in *cln3*^{-/-} optic nerve (0.136 ± 0.004 axons/ μm^2) compared with wild-type (0.212 ± 0.006 axons/ μm^2 ; $t_{(30)} = 9.34$, $P < 0.01$). Samples of axonal density represent the number of $50\text{-}\mu\text{m}^2$ areas containing a given axon density (B). The diameter of axons in *cln3*^{-/-} optic nerve (1.533 ± 0.049 μm) was greater than in wild-type optic nerve (mean = 1.262 ± 0.049 μm ; $t_{(60)} > 100,000$, $P < 0.01$). An equal number of axons ($n = 50$) were measured in multiple samples of wild-type and *cln3*^{-/-} nerve to account for differences in axon density.

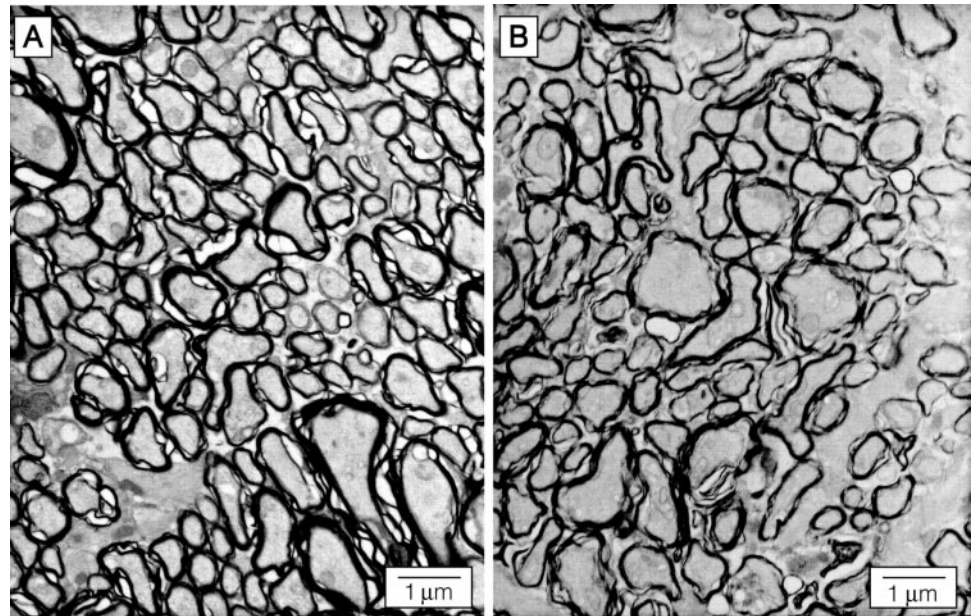


FIGURE 4. Myelin sheathing on individual axons was disrupted in the *cln3*^{-/-} optic nerve. (A, B) Electron micrographs of optic nerve from wild-type (A) and *cln3*^{-/-} (B) mice. (C) The thickness of myelin surrounding axons in *cln3*^{-/-} mice was significantly reduced: $0.06 \pm 0.001 \mu\text{m}$ in *cln3*^{-/-} versus $0.0882 \pm 0.001 \mu\text{m}$ in wild-type ($t_{(4138)} = 18.02$, $P < 0.01$). To measure myelin thickness, a montage of adjacent square grids of $5 \mu\text{m}$ per side were overlaid on the electron micrographs. Width measurements for myelin sheathing were obtained every time a grid line encountered myelin. For most axons, two encounters were measured. Magnification, $\times 7000$.

wild-type optic nerve. Spacing between axons of *cln3*^{-/-} optic nerve increases to give an overall impression of loose axonal packing, which suggests loss of axons (Fig. 2B). Comparison of axon density in *cln3*^{-/-} and wild-type specimens confirmed loss of axons in the *cln3*^{-/-} optic nerve (Fig. 3A). This decrease in density is not due to simple enlargement or swelling of the *cln3*^{-/-} optic nerve, because our measurements of cross-sectional area indicate that the nerve actually decreased in size. When differences in axonal density were taken into consideration, *cln3*^{-/-} optic nerve also contained fewer axons of small diameter than wild-type optic nerve (note the first bin in the histogram of Fig. 3B). Based on these results, we propose two possible mechanisms for axonal loss in the *Cln3*-deficient optic nerve. First, axonal loss is heterogeneous and accompanied by axonal hypertrophy (note the third and fourth bins in Fig. 3B). Alternatively, axonal loss associated with the absence of *Cln3* could target small diameter axons exclusively; however, to date, there is no evidence that small diameter axons are more vulnerable to disease resulting from the absence of *Cln3*. Our findings are consistent with optic nerve atrophy noted in patients with Batten disease¹⁹ and Tay-Sachs disease (variant B), another pediatric neurodegenerative disorder characterized by abnormal lipid storage.²⁵

Reduction in Myelin Thickness

Individual axons within the *cln3*^{-/-} optic nerve exhibit distention and distortion that results in a departure from the circular morphology of normal axons (Fig. 2B). Loss of uniformity at the level of individual axons is likely to underlie the eventual loss of axons in *cln3*^{-/-} optic nerve. Electron microscopy revealed a reduction in thickness of myelin surrounding axons of the *cln3*^{-/-} optic nerve (Figs. 4A-4C). No significant differences exist between myelin measurements in the peripheral and central portions of the *cln3*^{-/-} optic nerve, suggesting that the reduction in myelin thickness is heterogeneous. Although loss of myelin surrounding the optic nerve has not yet been noted in human Batten disease, myelin loss in the optic nerve is consistent with advanced Tay-Sachs disease (variant B).²⁵

Cln3 Protein Expression in Optic Nerve

To reliably associate optic nerve disease with loss of *Cln3*, we assayed *Cln3* expression in brain, retina and optic nerve across multiple species. Our results indicate that *Cln3* protein is highly conserved between species and between different CNS structures, including brain, retina, and optic nerve (Figs. 5A-

5C). To the best of our knowledge, our work is the first to report expression of Cln3 in optic nerve of any species, as well as the first to demonstrate Cln3 expression in a nonhuman primate. The presence of Cln3 in primate retina and optic nerve suggests the optic nerve as a likely target of degeneration induced by CLN3 dysfunction in humans.

Developmental Hypothesis for Optic Nerve Degeneration

It is unclear whether the reduction in myelination noted herein is evidence of abnormal development or evidence of a degenerative mechanism. We propose a developmental hypothesis for reduced myelination based on the possible role of CLN3 in pH homeostasis (Fig. 6). Myelination depends in part on the generation of oligodendrocytes. The oligodendrocyte-type 2 astrocyte precursor (O-2A) cell can differentiate to produce a type-II astrocyte or an oligodendrocyte (oligo).²⁶ However, the O-2A cell can also follow a self-renewal pathway to form additional O-2A cells.²⁶ Extracellular signals can induce both differentiation²⁷ and self-renewal of O-2A cells.²⁸ Although extracellular signals play a major role in O-2A cell fate, intracellular factors, particularly redox state, also appear to be important. Specifically, an oxidized state drives differentiation of O-2A cells, while a reduced state perpetuates O-2A self-renewal.²⁷ Therefore, intracellular events, like alterations in intracellular pH, that alter redox state may also influence cell fate. Although the specific function of CLN3 is unknown, the protein may play a role in pH homeostasis.^{15,16} Low intracellular pH, such as that reported in the yeast model of Batten disease, may produce an overall state of reduction in cells expressing irregular CLN3. Given the relationship between O-2A cell fate and the redox state, irregularities in CLN3 function may promote O-2A self-renewal, thereby reducing the production of oligodendrocytes and leading to a subsequent decrease in myelin. Although Cln3 expression in O-2A cells has not yet been investigated, disruption of developmental processes at the level of precursor cells is an intriguing possible mechanism for neurodegeneration in Batten disease.

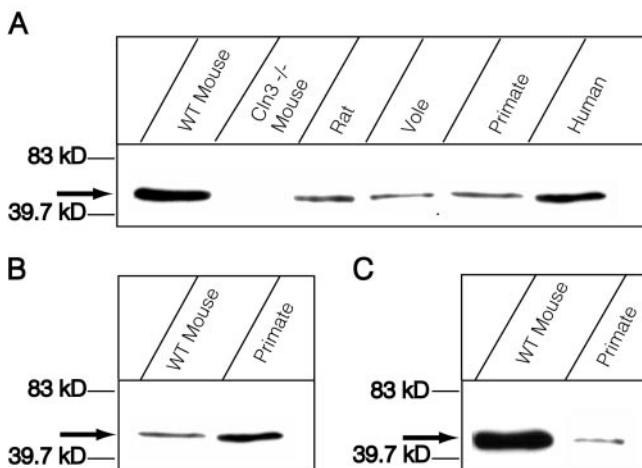


FIGURE 5. Cln3 protein was highly conserved between species and between the different central nervous system (CNS) structures. (A) Western blot demonstrated Cln3 expression in brain. Lanes (left to right): wild-type mouse, *cln3*^{-/-} mouse, rat, vole, primate, and human. (B) Western blot of mouse and primate retina. Lanes, left to right: wild-type mouse and primate. (C) Western blot of mouse and primate optic nerve. Lanes, left to right: wild-type mouse and primate. Arrows: expected molecular weight of Cln3 (48 kDa).

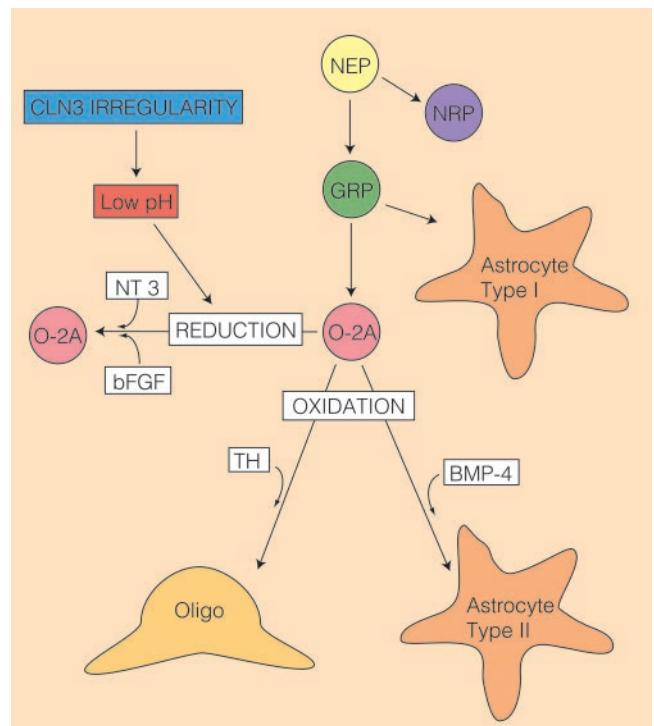


FIGURE 6. Schematic model of how developmental disruptions of myelination in *cln3*^{-/-} optic nerve may contribute to its disease. Myelination depends, in part, on the generation of oligodendrocytes. Briefly, neuroepithelial stem cells (NEP) can produce either a glial-restricted precursor (GRP) or a neuron-restricted precursor (NRP).²⁶ Following the glia-genesis pathway, GRP may produce either a type-I astrocyte or a second progenitor cell, the oligodendrocyte-type 2 astrocyte precursor cell (O-2A).²⁶ At this junction, the O-2A cell can differentiate to produce a type-II astrocyte or an oligodendrocyte (oligo).²⁶ However, the O-2A cell can also follow a self-renewal pathway to form additional O-2A cells.²⁶ Extracellular signals such as thyroid hormone (TH) and bone morphogenic protein (BMP)-4 can induce differentiation of O-2A cells to form oligodendrocytes and type-II astrocytes, respectively.²⁷ Likewise, basic fibroblast growth factor (bFGF) and neurotrophin (NT)-3 can induce O-2A self-renewal.²⁸ Intracellular factors, particularly the redox state, also appear to be important in O-2A cell fate. An oxidized state drives differentiation of O-2A cells, whereas a reduced state perpetuates O-2A self-renewal.²⁷ In cells expressing irregular CLN3, low intracellular pH may produce an overall state of reduction in cells; thereby promoting O-2A self-renewal and reducing the production of oligodendrocytes.

Acknowledgments

The authors thank Karen Bentley for electron microscopy services.

References

- Hall NA, Lake BD, Dewji NN, Patrick AD. Lysosomal storage of subunit c of mitochondrial ATP synthase in Batten's Disease (ceroid lipofuscinosis). *Biochem J.* 1991;275:269-272.
- Palmer DN, Fearnley IM, Walker JE, et al. Mitochondrial ATP synthase subunit c storage in the ceroid lipofuscinoses (Batten disease). *Am J Med Gen.* 1992;42:561-567.
- Hughes SM, Rawson-Moroni P, Jolly RD, Jordan TW. Submitochondrial distribution and delayed proteolysis of subunit c of the H⁺-transporting ATP-synthase in ovine ceroid lipofuscinosis. *Electro-physiosis.* 2001;22:1785-1794.
- Janes RW, Munroe PB, Mitchison HM, Gardiner M, Mole SE, Wallace BA. A model for Batten disease protein CLN3: Functional implications from homology and mutations. *FEBS Lett.* 1996;399:75-77.

5. Kaczmarek W, Wisniewski KE, Golabek A, Kaczmarek A, Kida E, Michalewski M. Studies of membrane association of CLN3 protein. *Mol Gen Metabol.* 1999;66:261-264.
6. Katz ML, Gao CL, Prabhakaram M, Shibuya H, Liu P, Johnson GS. Immunocytochemical localization of the Batten disease (CLN3) protein in retina. *Invest Ophthalmol Vis Sci.* 1997;38:2375-2386.
7. Järvelä I, Sainio M, Rantamäki T, et al. Biosynthesis and intracellular targeting of the CLN3 protein defective in Batten disease. *Hum Mol Genet.* 1998;7:85-90.
8. Golabek AA, Kaczmarek W, Kida E, Kaczmarek A, Michalewski MP, Wisniewski KE. Expression studies of CLN3 protein (Battenin) in fusion with the green fluorescent protein in mammalian cells in vitro. *Mol Gen Metabol.* 1999;66:277-282.
9. Kida E, Kaczmarek W, Golabek AA, Kaczmarek A, Michalewski M, Wisniewski KE. Analysis of intracellular distribution and trafficking of the CLN3 protein in fusion with the green fluorescent protein in vitro. *Mol Genet Metabol.* 1999;66:265-271.
10. Kremmidiotis G, Lensik IL, Bilton RL, et al. The Batten disease gene product (CLN3p) is a golgi integral membrane protein. *Hum Mol Genet.* 1999;8:523-531.
11. Margraf LR, Boriack RL, Routhout AAJ, et al. Tissue expression and subcellular localization of CLN3, the Batten disease protein. *Mol Genet Metab.* 1999;66:283-289.
12. Järvelä I, Lehtovirta M, Tikkanen R, Kytälä A, Jalanko A. Defective intracellular transport of CLN3 is the molecular basis of Batten disease (JNCL). *Hum Mol Genet.* 1999;8:1091-1098.
13. Haskell RE, Carr CJ, Pearce DA, Bennett MJ, Davidson BL. Batten disease: evaluation of CLN3 mutations on protein localization and function. *Hum Mol Genet.* 2000;9:735-744.
14. Chattopadhyay S, Ito M, Cooper JD, et al. An autoantibody inhibitory to glutamic acid decarboxylase in the neurodegenerative disorder Batten disease. *Hum Mol Genet.* 2002;11:1421-1431.
15. Pearce DA. Experimental models of NCL: the yeast model. *Adv Genet.* 2001;45:205-216.
16. Holopainen JM, Saarikoski J, Kinnunen PKJ, Järvelä I. Elevated lysosomal pH in neuronal ceroid lipofuscinoses (NCLs). *Eur J Biochem.* 2001;268:5851-5856.
17. Bensaoula T, Shibuya H, Katz ML, Smith JE, Johnson GS, John SK, Milam AH. Histopathologic and immunocytochemical analysis of the retina and ocular tissues in Batten disease. *Ophthalmology.* 2000;107:1746-1753.
18. Goebel HH, Mole SE, Lake BD. The neuronal ceroid lipofuscinosis (Batten Disease). *Biomed Health Res.* 1999;33:55-76.
19. Spalton DJ, Taylor DSI, Sanders MD. Juvenile Batten's disease: an ophthalmological assessment of 26 patients. *Br J Ophthalmol.* 1980;64:726-732.
20. Seigel GM, Lotery A, Kummer A, et al. Retinal pathology and function in a CLN3 knockout mouse model of juvenile neuronal ceroid lipofuscinosis (Batten disease). *Mol Cell Neurosci.* 2002;19:515-527.
21. Greene NDE, Bernard DL, Taschner PEM, et al. A murine model for juvenile NCL: gene targeting of mouse CLN3. *Mol Genet Metab.* 1999;66:309-313.
22. Porter KR, Bonneville MA. *Fine Structures of Cells and Tissues.* 4th ed. Philadelphia, PA: Lea and Febiger; 1973:134-136.
23. Ross MH, Romrell LJ. *Histology: A Text and Atlas.* 2nd ed. Baltimore: Williams & Wilkins; 1989:96-97.
24. Chattopadhyay S, Kriscenski-Perry E, Wenger DA, Pearce DA. An autoantibody to GAD65 in sera of patients with juvenile neuronal ceroid lipofuscinoses. *Neurology.* 2002;59:1816-1817.
25. Volk BW, Adachi M, Schneck L. The gangliosidoses. *Hum Patbol.* 1975;6:555-569.
26. Noble M, Dietrich J. Intersections between neurobiology and oncology: tumor origin, treatment and repair of treatment-associated damage. *Trends Neurosci.* 2002;25:103-107.
27. Smith J, Ladi E, Proschel-Mayer M, Noble M. Redox state is a central modulator of the balance between self-renewal and differentiation in a dividing glial precursor cell. *Proc Natl Acad Sci USA.* 2000;97:10032-10037.
28. Böglér O, Wren D, Barnett SC, Land H, Noble MD. Cooperation between two growth factors promotes extended self-renewal and inhibits differentiation of oligodendrocyte-type 2 astrocyte (O-2A) progenitor cells. *Proc Natl Acad Sci USA.* 1990;87:6368-6372.